IOPscience iopscience.iop.org

Home Search Collections Journals About Contact us My IOPscience

Optical amplification of Raman scattering in a GaAs bulk microcavity

This article has been downloaded from IOPscience. Please scroll down to see the full text article.

1998 J. Phys.: Condens. Matter 10 9535

(http://iopscience.iop.org/0953-8984/10/42/018)

View the table of contents for this issue, or go to the journal homepage for more

Download details:
IP Address: 171.66.16.210
The article was downloaded on 14/05/2010 at 17:38

Please note that terms and conditions apply.

J. Phys.: Condens. Matter **10** (1998) 9535–9540. Printed in the UK PII: S0953-8984(98)93374-4

Optical amplification of Raman scattering in a GaAs bulk microcavity

A Mlayah†, O Marco†, J R Huntzinger†, A Zwick†, R Carles†,
V Bardinal‡, C Fontaine‡ and A Muñoz-Yagüe‡

† Laboratoire de Physique des Solides, ESA 5477, Université Paul Sabatier, 118 route de Narbonne, 31062 Toulouse Cédex, France
‡ Laboratoire d'Analyse et d'Architecture des Systèmes, UPR 8001 CNRS, 7 avenue du colonel Roche, 31077 Toulouse Cédex, France

Received 14 April 1998

Abstract. We present photoluminescence, reflectivity and Raman scattering measurements on a GaAs Fabry–Pérot bulk microcavity. A strong enhancement of the Raman scattering efficiency is observed when either the incident or the scattered photons are tuned to the cavity mode. Resonance curves are obtained for scattering by both transverse and longitudinal optical phonons, and analysed in terms of the optical amplification due to confinement of the electromagnetic field. Resonance effects as strong as that observed in microcavities with embedded quantum wells are observed. Single and double resonance Raman profiles are calculated and a good agreement with measurements is obtained.

1. Introduction

Fabry–Pérot semiconductor microcavities receive a growing interest due to their application potential in opto-electronics as high efficiency emitters, optical routing systems and thresholdless lasing devices [1]. From a fundamental point of view microcavity structures introduce in solid state physics the concept of photon confinement and hence the ability to control the photonic density of states [2, 3]. Indeed, the reduction of the continuum of photon states to a few (or one) allowed electromagnetic modes has important impacts on the light–matter interaction: enhancement (or inhibition) of the spontaneous emission, strong exciton–photon coupling [4–8]. Moreover, it has been shown that microcavity structures can be used as optical resonators for inelastic light scattering.

Previously published studies devoted to Raman scattering enhancement by means of photon confinement in a semiconductor microcavity were performed on Fabry–Pérot structures with quantum wells embedded inside the cavity [9–14]. Fainstein *et al* [9–11] first reported the observation of resonant Raman scattering by interface phonons in InGaAs/GaAs quantum wells embedded in a $\lambda/2$ AlAs cavity. Moreover, Raman scattering has been studied in the strong exciton–photon coupling regime, and clear evidence for cavity polariton mediation of the scattering processes has been indicated [12–14]. In this work we present photoluminescence, reflectivity and Raman scattering measurements on a GaAs bulk microcavity where the whole body of the cavity is used as the active material [15]. In this structure the energy separation between the Fabry–Pérot mode and the excitonic transitions is such that strong exciton–photon coupling effects are ruled out. In that way pure photonic effects can be investigated. The photoluminescence and reflectivity data are

0953-8984/98/429535+06$19.50 © 1998 IOP Publishing Ltd

here used to study the optical properties of the cavity around the Fabry–Pérot resonance and to determine the experimental configurations for which the enhancement of Raman scattering can be achieved. Resonance profiles are obtained for Raman scattering by both transverse and longitudinal optical phonons and analysed in terms of optical amplification effects.

2. Experiments

The sample used in this study is an asymmetric Fabry–Pérot resonator grown by molecular beam epitaxy on a (100) GaAs substrate. It consists of a $(6\lambda/2)$ GaAs cavity sandwiched between two distributed Bragg reflectors (DBRs). The top DBR is made of nine quarter-wave $Al_{0.1}Ga_{0.9}As/AlAs$ stacks, whereas the bottom DBR involves 24 stacks in order to correct the backside reflection for the absorption in the GaAs cavity. Absence of rotation during growth leads to a wedge-shaped sample: the thickness of all layers varies by 3% from the centre to the border of the wafer, and thus the cavity mode energy depends on the position on the sample. This allows us to tune the cavity mode either to the incident or to the scattered photons by selecting the appropriate point under investigation.

All measurements were performed at liquid nitrogen temperature. The photoluminescence (PL) and Raman scattering (RS) were excited by focusing, onto a 0.1 mm diameter spot, a 4 mW beam of a Ti:Sa laser operating at $E_L = 1.478$ eV, i.e. below the band-gap of GaAs ($\approx$1.51 eV at 77 K). The angle of incidence was fixed at $\theta_i = 50°$ with respect to the cavity axis. The emitted light was collected along the cavity axis $\theta_d = 0°$ and dispersed using a triple spectrometer coupled to a conventional photon counting system. In our experimental configuration only the laser spot position was changed (simply by moving the sample). In addition to the PL and RS data, the intensity of the reflected laser beam was measured for each probed point.

3. Results and discussion

A typical photoluminescence spectrum is shown in figure 1. The strong recombination peak located at $E_L - E_d = 31$ meV ($E_L - E_d$ being the energy shift between incident and detected photons) is due to the spontaneous emission of photons into the cavity mode acting as a band-pass filter. Since the emitted light is detected along the cavity axis one obtains from this spectrum the cavity mode energy: $E_c(\theta) = E_c(0) = 1.447$ eV. The energy width $\Delta E_c(0)$ of the cavity mode is estimated at 2.4 meV from the linewidth of the filtered luminescence peak. In principle, one has to correct the PL spectrum of figure 1 from the PL response of bulk GaAs (i.e. without cavity) in order to derive $E_c(0)$ and $\Delta E_c(0)$. Nevertheless, here the energy range under consideration is well below the excitonic transitions ($\approx$1.51 eV) and hence the photoluminescence intensity (of bulk GaAs) is a slowly varying function of energy. So, accurate values of $E_c(0)$ and $\Delta E_c(0)$ can be deduced directly from the filtered PL spectrum.

The quality factor of the cavity, defined by $Q(0) = E_c(0)/\Delta E_c(0)$, is around 600 for the investigated point. By probing different points we found that $E_c(0)$ and $\Delta E_c(0)$ vary by 1 meV mm^{-1} and 50 μeV mm^{-1}, respectively. The change of the filtered PL intensity with point position is of particular interest: a plot of the maximum intensity (i.e. at $E_d = E_c(0)$) of the filtered PL versus the detuning $E_L - E_c(0)$ between the incident photons and the cavity mode (at $\theta = 0$) is presented in figure 1. The thus-obtained curve is a PL excitation (PLE) spectrum but instead of changing the excitation energy (E_L) as usual, here E_L is kept fixed

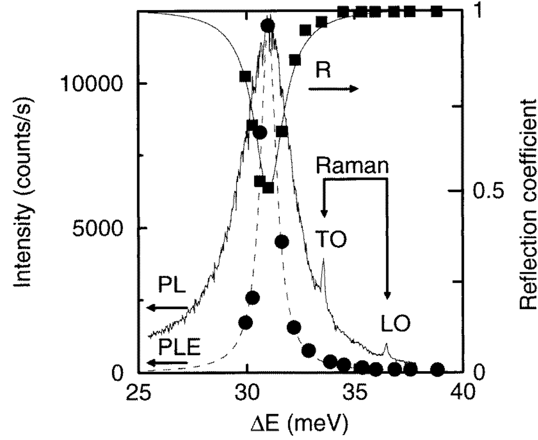

Figure 1. PL, PLE, reflectivity (R) and Raman measurements. The PL spectrum is plotted as a function of the energy shift $\Delta E = E_L - E_d$ between incident and detected photons. The lines labelled TO and LO are due to Raman scattering by transverse and longitudinal optical phonons, respectively. The reflectivity (R) and PLE curves are plotted as a function of the detuning $\Delta E = E_L - E_c(0)$ between the incident photons and the cavity mode at $\theta = 0°$. The continuous line is the best fit of $1 - T_L$ to the reflectivity data. The dashed line is a guide to the eye.

and the cavity mode energy $E_c(0)$ is varied by probing different points. This curve shows a maximum emission of PL at $E_L - E_c(0) = 31$ meV corresponding to a particular point of the sample where absorption of the incident photons is maximum. This is corroborated by the reflectivity measurements (figure 1). As a matter of fact, the intensity of the reflected laser beam is minimum also for $E_L - E_c(0) = 31$ meV. So, the correlation between the PLE and reflectivity data reveals the point of the sample where a maximum of incident photons are transmitted to the cavity. This situation occurs under resonant excitation of the cavity, i.e. for zero detuning $E_L - E_c(50)$ between the incident photons and the cavity mode at $\theta = 50°$ (angle of incidence). One can note in figure 1 that the peak intensity and energy of the filtered PL spectrum coincide with those of the PLE curve. In fact, the PL spectrum shown in figure 1 was excited in resonance with the cavity mode, i.e. at $E_L = E_c(50)$. Then, we obviously deduce $E_c(50) - E_c(0) = 31$ meV for the energy difference between the cavity mode at $\theta = 0°$ and $\theta = 50°$. According to the angular dispersion of the cavity mode, $E_c(\theta) = E_c(0)/\sqrt{1 - \sin^2(\theta)/n^2}$ (where $n \approx 3.7$ is the effective optical index), the energy difference $E_c(50) - E_c(0)$ can be approximated by $E_c(0)\sin^2(50)/2n^2$. Then, since $E_c(0)$ varies by 1 meV mm^{-1}, the change of $E_c(50) - E_c(0)$ with point position on the sample is estimated at 20 μeV mm^{-1} only, and thus $E_c(50) - E_c(0)$ can be assumed constant.

Stokes Raman scattering by transverse (TO) and longitudinal (LO) optical phonons of GaAs is visible on the low energy tail of the filtered PL spectrum at $E_{TO} = 33$ meV and $E_{LO} = 36$ meV, respectively (figure 1). As mentioned above, this spectrum corresponds to the incoming resonance situation. Resonant Raman scattering in the outgoing channel is achieved by tuning the cavity mode to the scattered photons: $E_c(0) = E_d = E_L - E_{TO}$ (or $E_L - E_{LO}$). Figure 2 presents a set of typical Raman spectra obtained for $E_c(0) = E_L - E_{TO}$ (spectrum a), $E_L - E_{TO} < E_c(0) < E_L - E_{LO}$ (spectrum b), $E_c(0) = E_L - E_{LO}$ (spectrum c) and for the out of resonance situation $E_c(0) > E_L - E_{LO}$ (spectrum d). A strong

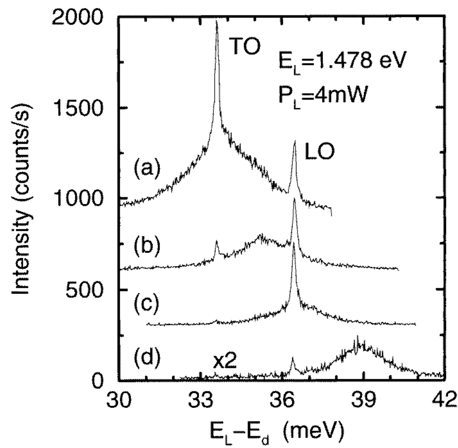

Figure 2. Resonant Raman spectra obtained for $E_c(0) \approx E_L - E_{TO}$ (spectrum a), $E_L - E_{TO} < E_c(0) < E_L - E_{LO}$ (spectrum b), $E_c(0) \approx E_L - E_{LO}$ (spectrum c) and out of resonance $E_c(0) > E_L - E_{LO}$ (spectrum d).

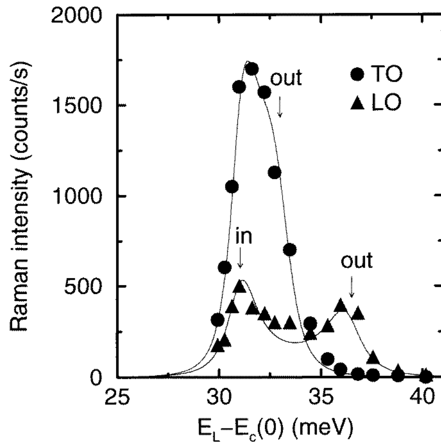

Figure 3. Comparison between measured (symbols) and calculated (continuous lines) resonance profiles for Raman scattering by TO (dots) and LO (triangles) phonons. The intensities are plotted as a function of the detuning between the incident photons and the cavity mode at $\theta = 0°$. The arrows indicate the location of the incoming and outgoing resonance.

enhancement of the scattering by both LO and TO phonons can be observed in spectra a and c (in comparison with spectrum d). Of course for outgoing resonance the filtered PL falls into the energy range of Raman scattering and is visible in spectra a, b and c as a broad band on which the phonon lines are superimposed. In order to derive accurate values of the cavity mode energy $E_c(0)$ and width $\Delta E_c(0)$, as well as of the Raman intensities, we used a deconvolution of the measured spectra into three Lorentzian components (TO, LO lines and PL band).

Figure 3 shows a plot of the LO and TO intensities versus the detuning $E_L - E_c(0)$. These data point out the enhancement of Raman scattering for both incoming and outgoing resonance with the cavity mode. Indeed, according to the PLE and reflectivity measurements

shown in figure 1, incoming resonance occurs at $E_L = E_c(50) = E_c(0) + 31$ meV and one can see in figure 3 that both TO and LO intensities indeed exhibit a maximum at $E_L - E_c(0) \approx 31$ meV. With increasing detuning the Raman intensities decrease and then a second maximum is observed but only for scattering by LO phonons which corresponds to the outgoing resonance $E_L - E_{LO} = E_c(0)$ i.e. $E_L - E_c(0) = 36$ meV. In fact, for scattering by TO phonons incoming and outgoing resonance are not resolved. Indeed, since $E_{TO} = 33$ meV, the energy shift between incoming, $E_L - E_c(0) = 31$ meV, and outgoing, $E_L - E_c(0) = 33$ meV, resonance is only 2 meV which is close to the energy width of the cavity mode. In other words, Raman scattering by TO phonons is rather doubly resonant.

Figure 3 also presents resonance Raman profiles calculated assuming the measured intensities are proportional to $T_L T_s$, where T_L (T_s) is the transmission coefficient of the cavity at the incident (scattered) photon energy [9, 10]. This simply means that in order to observe a Raman process the incident photon has to come into the cavity, then interacts with optical phonons (via electron–phonon coupling) and finally leaves the cavity. For T_L and T_s we choose Lorentzian functions located respectively at $E_c(50)$ (incoming resonance) and $E_c(0)$ (outgoing resonance). As mentioned above, $E_c(50) - E_c(0)$ is assumed constant (i.e. independent of $E_c(0)$). Strictly speaking the linewidths $\Delta E_c(50)$ and $\Delta E_c(0)$, of respectively T_L and T_s, should change with $E_c(0)$ since the absorption coefficient of the GaAs active layer contributes to the damping of the cavity mode and is energy dependent. However, we found that $\Delta E_c(0)$ varies by only 50 μeV mm^{-1}, obviously because $E_c(0)$ (and also $E_c(50)$) is in the energy range where the absorption coefficient of GaAs weakly depends on energy. Therefore, we assume constant $\Delta E_c(50)$ and $\Delta E_c(0)$ and determine these values using a fit of $1 - T_L$ to the reflectivity data (figure 1), and of T_s to the filtered PL spectrum labelled b in figure 2 (i.e. close to the outgoing resonance). We thus deduce $\Delta E_c(50) = 1.8$ meV and $\Delta E_c(0) = 2.1$ meV. Note that this last value is smaller than the one deduced from the filtered PL data of figure 1 ($\Delta E_c(0) = 2.4$ meV) because of the lower absorption coefficient; indeed in figure 2, $E_c(0)$ is shifted toward lower energies (with respect to figure 1).

As can be observed in figure 3, a good agreement between the calculated and measured resonance Raman profiles is obtained for both TO and LO phonon scattering. It is worthwhile to underline that the same values of $\Delta E_c(50)$ and $\Delta E_c(0)$ are used for the calculations of the TO and LO phonon resonance curves. Note that there is no adjustable parameter except the scaling factors $S_{LO(TO)}$. The ratio S_{TO}/S_{LO} deduced from the data of figure 3 is around 0.5. Nevertheless, the enhancement of the Raman efficiency is much more pronounced for scattering by TO phonons because of the double resonance effect already discussed above.

According to the Raman selection rules for a (100) oriented GaAs face [16, 17], only LO phonons may take part in the backscattering of the incident light. However, it is well known that deviations from the true backscattering configuration lead to a partial activation of TO phonons [16]. But even for excitation under a grazing incidence the TO/LO intensity ratio, measured on a thick GaAs layer (without cavity), does not exceed 0.1. Here, we found a larger value: $S_{TO}/S_{LO} \approx 0.5$. This can be explained by the fact that a cavity gives the possibility of observing not only the backward but also the forward scattering of light via a Raman process. Indeed, when the incident (scattered) photons are in resonance with the cavity mode the bottom mirror of the cavity acts as a light source (a light detector). So, the wavevector of the emitted phonon can be not only along the [100] direction (near backscattering) but also along the [110] direction (near forward scattering) for which scattering by TO phonons is allowed [16, 17]. This cavity effect may be responsible for the activation of the TO phonon scattering as already proposed by Fainstein *et al* [9, 10].

The intensity gain due to the confinement of the electromagnetic field can be estimated by considering the photon density of states around the Fabry–Pérot resonance. Indeed, the cavity thickness along the growth direction is $L_c = 6\lambda/2$ and for a given polarization there is one photon mode in the frequency range $\Delta E_c(0)$ around $E_c(0)$. So the one-dimensional density of states is essentially $1/(\Delta E_c(0) L_c) = Q(0)/3(hc)^{-1}$, where Q is the quality factor of the cavity and $(hc)^{-1}$ is the photon density of states in the case of free propagation [2]. For our cavity the enhancement factor $Q(0)/3$ is around 200. So the Raman intensity gain should be of the order of 4×10^4 assuming the same enhancement factors for both the incoming and outgoing resonance. As a matter of fact, without a cavity, the Raman signal of a GaAs thick layer probed under the same experimental conditions (laser power, laser photon energy, temperature, accumulation time, ...) could not emerge from the background noise which is around 5 counts s^{-1}. The intensity scale in figures 2 and 3 is indicative of the large optical gain.

4. Conclusion

In summary we have studied the enhancement of Raman scattering near the Fabry–Pérot resonance of a bulk microcavity. Single and double resonance effects were observed for Raman scattering by TO and LO phonons. The energy and linewidth of the resonance, for the incoming and outgoing channels, were determined from the reflectivity and photoluminescence measurements, and then used to analyse quantitatively the resonance Raman profiles.

In structures with quantum wells embedded inside the cavity the energy of the Fabry–Pérot mode is usually well below the band gap of the barrier material. So, since absorption occurs only in the quantum well region, large quality factors can be easily achieved and strong resonance effects are observed [9–11]. In our structure, absorption takes place in the whole body of the cavity which is a serious limitation of the quality factor. Nevertheless, we have shown that in bulk microcavities, even when the Fabry–Pérot mode energy is close to but below the absorption edge of the active material, resonance Raman scattering as strong as that observed in microcavities with QWs can be obtained.

References

[1] Burstein E and Weisbuch C (ed) 1995 *Confined Electrons and Photons: New Physics and Applications* (New York: Plenum)
[2] Kleppner D 1981 *Phys. Rev. Lett.* **47** 233
[3] Yablonovitch E 1987 *Phys. Rev. Lett.* **58** 2059
[4] Weisbush C, Nishioka M, Ishikawa A and Arakawa Y 1992 *Phys. Rev. Lett.* **69** 3314
[5] Stanley R P, Houdré R, Oesterle U and Illegems M 1994 *Appl. Phys. Lett.* **65** 2093
[6] Abram I, Lung S, Kuszelewicz R, Le Roux G, Licoppe C, Oudar J L, Rao E V K, Bloch J I, Planel R and Thierry-Mieg V 1994 *Appl. Phys. Lett.* **65** 2516
[7] Fisher T A, Afshar A M, Whittaker D M and Skolnick M S 1995 *Phys. Rev.* B **51** 2600
[8] Tredicucci A, Chen Y, Pellegrini V and Deparis C 1995 *Appl. Phys. Lett.* **66** 2388
[9] Fainstein A, Jusserand B and Thierry-Mieg T 1995 *Phys. Rev. Lett.* **75** 3764
[10] Fainstein A, Jusserand B and Thierry-Mieg V 1996 *Phys. Rev.* B **53** R13287
[11] Fainstein A, Jusserand B and Thierry-Mieg V 1996 *Phys. Rev.* B **54** 11505
[12] Fainstein A, Jusserand B and Thierry-Mieg V 1997 *Phys. Rev. Lett.* **78** 1576
[13] Tribe W R, Baxter D, Skolnik M S, Mowbray D J, Fisher T A and Roberts J S 1997 *Phys. Rev.* B **56** 12429
[14] Pau S, Björk G, Cao H, Tassone F, Huang R, Yamamoto Y and Stanley R P 1997 *Phys. Rev.* B **55** R1942
[15] Chen Y, Tredicucci A and Bassani F 1995 *Phys. Rev.* B **52** 1800
[16] Puech P, Landa G, Carles R, Pizani P, Danran E and Fontaine C 1994 *J. Appl. Phys.* **76** 2773
[17] Poulet H and Mathieu J P 1970 *Spectres de Vibration et Symétries des Cristaux* (London: Gordon and Breach)